N87-22205

STATIC AND DYNAMIC CHARACTERISTICS OF PARALLEL-GROOVED SEALS

Takuzo Iwatsubo
Kobe University
Rokko, Nada, 657, Japan

Bo-suk Yang
The National Fisheries University of Pusan
599, Daeyon-dong, Nam-ku, Pusan, Korea

Ryuji Ibaraki
Toyota Motor Corporation
1, Toyota-cho, Toyota, 471, Japan

This paper presents an analytical method to determine static and dynamic characteristics of annular parallel-grooved seals. The governing equations were derived by using the turbulent lubrication theory based on the law of fluid friction. Linear zero- and first-order perturbation equations of the governing equations were developed, and these equations were analytically investigated to obtain the reaction force of the seals. An analysis is presented that calculates the leakage flow rate, the torque loss, and the rotordynamic coefficients for parallel-grooved seals. To demonstrate this analysis, we show the effect of changing number of stages, land and groove width, and inlet swirl on stability of the boiler feed water pump seals. Generally, as the number of stages increased or the grooves became wider, the leakage flow rate and rotordynamic coefficients decreased and the torque loss increased.

INTRODUCTION

Annular pressure seals can significantly influence the dynamic behavior of rotating machinery by the presence of a high-pressure difference in the close clearance spaces of the leakage path.

Black and Jenssen (refs. 1 to 3) have explained the influence of seal forces on the rotordynamic behavior of pumps. Childs has analyzed the short seal (ref. 4) and has made finite-length analyses (ref. 5) based on Hirs' governing equation, which yields an analytical expression for the seal dynamic coefficients incorporating all of Black and Jenssen's various developments.

Although these results apply only for small seal motion about a centered position, Allaire, et al. (ref. 6), the authors (ref. 7) have expanded these analyses to calculate dynamic coefficients at large eccentricities.

Fleming (ref. 8) has developed an analysis for gas seals with a constant clearance or with convergently tapered geometries. Child (ref. 9) investigated dynamic coefficients for convergently tapered seals both analytically and experimentally.

Previous analytical and experimental developments have generally examined dynamic characteristics of the annular straight seal and the tapered seal. But the dynamic characteristics of the parallel-grooved seal have not been analyzed theoretically. Bolleter (ref. 10) experimentally investigated stability limits for balance pistons with two different types of serration. He showed that serrations that are deep and wide prevent seizure.

In this paper the static and dynamic characteristics of the multistage parallel-grooved seal operating within the turbulent flow region are analyzed theoretically with consideration of the inertia effect. The present analysis combines the previous analysis of the straight seal with the analysis of the labyrinth seal performed by the authors. Namely, land analysis is used for the straight seal and groove analysis is used for the labyrinth seal.

SYMBOLS

C_{lo}	nominal seal radial clearance, cm
C_{xx}, C_{yx}	seal damping coefficients, N s/m
D	journal diameter, cm
F	fluid force, N
H	seal radial clearance, cm
K_{xx}, K_{yx}	seal stiffness coefficients, N/m
L	seal length, cm
L_l	land width, cm
lg	groove width, cm
M_{xx}, M_{yy}	seal add mass coefficients, N s^2/m
MG	fluid mean depth, cm
P	fluid pressure, MPa
Q	rate of leakage, m^3/s
R	seal radius, cm
R_a	axial Reynolds number
R_r	circumferential Reynolds number
S	number of stages
T	groove depth, cm
t	time, s

Torq	torque, N m
u,w	tangential and axial fluid velocity components, m/s
V	journal surface velocity, m/s
x	circumferential coordinate
y	radial coordinate
z	axial coordinate
ε	small eccentricity ratio
θ	diverging angle of stream behind land section
λ	friction loss coefficient
μ	fluid viscosity, mPa s
ν	fluid kinematic viscosity, m^2/s
ξ	loss coefficient
ρ	fluid density, kg/m^3
τ	shear stress, Pa
ω	journal angular velocity, rad/s

Subscripts:

a	axial direction
c	radial direction
d	groove defined in equation (13)
ex	exit
f	between clearance flow and cavity flow
g	groove
in	inlet
j	journal
ℓ	land
r	circumferential direction
s	casing

(•) d( )/dt

m mean

GOVERNING EQUATION AND ANALYSIS

Governing Equation

Figure 1 illustrates the geometry of the parallel-grooved seal. Under the usual assumptions for problems of throughflow across annuli with a fine clearance, the momentum and continuity equations are, respectively, as follows:

$$\rho\left\{\frac{\partial \bar{u}}{\partial t}+\bar{u}\frac{\partial \bar{u}}{\partial x}+\bar{w}\frac{\partial \bar{u}}{\partial z}\right\}=-\frac{\partial \bar{P}}{\partial x}+\mu\frac{\partial^2 \bar{u}}{\partial y^2}-\rho\frac{\partial \overline{u'v'}}{\partial y} \quad \text{(x-direction)} \tag{1}$$

$$\rho\left\{\frac{\partial \bar{w}}{\partial t}+\bar{u}\frac{\partial \bar{w}}{\partial x}+\bar{w}\frac{\partial \bar{w}}{\partial z}\right\}=-\frac{\partial \bar{P}}{\partial z}+\mu\frac{\partial^2 \bar{w}}{\partial y^2}-\rho\frac{\partial \overline{v'w'}}{\partial y} \quad \text{(z-direction)} \tag{2}$$

$$\frac{\partial \bar{u}}{\partial x}+\frac{\partial \bar{v}}{\partial y}+\frac{\partial \bar{w}}{\partial z}=0 \tag{3}$$

The fluid velocities u and w are integrated across the film and are transformed into the mean velocities u_m and w_m.

$$u_m=\frac{1}{H}\int_0^H \bar{u}\,dy \qquad w_m=\frac{1}{H}\int_0^H \bar{w}\,dy \qquad \int_0^H \frac{\partial \bar{w}}{\partial t}\,dy=\frac{\partial}{\partial t}\int_0^H \bar{w}\,dy=\frac{\partial}{\partial t}(Hw_m)$$

$$\int_0^H \bar{w}\frac{\partial \bar{w}}{\partial z}\,dy=\frac{\partial}{\partial z}\int_0^H \bar{w}^2\,dy=\frac{\partial}{\partial z}(\Gamma_{aa}Hw_m) \qquad \int_0^H \frac{\partial \bar{u}}{\partial t}\,dy=\frac{\partial}{\partial t}\int_0^H \bar{u}\,dy=\frac{\partial}{\partial t}(Hu_m)$$

$$\int_0^H \bar{u}\frac{\partial \bar{u}}{\partial x}\,dy=\frac{\partial}{\partial x}\int_0^H \bar{u}^2\,dy=\frac{\partial}{\partial x}(\Gamma_{rr}Hu_m^2) \qquad \int_0^H \frac{\partial \bar{u}}{\partial x}\,dy=\frac{\partial}{\partial x}\int_0^H \bar{u}\,dy=\frac{\partial}{\partial x}(Hu_m)$$

$$\int_0^H \bar{w}\frac{\partial \bar{u}}{\partial z}\,dy=\frac{\partial}{\partial z}\int_0^H \overline{wu}\,dy=\frac{\partial}{\partial z}(\Gamma_{ar}Hu_mw_m) \qquad \int_0^H \frac{\partial \bar{w}}{\partial z}\,dy=\frac{\partial}{\partial z}\int_0^H \bar{w}\,dy=\frac{\partial}{\partial z}(Hw_m)$$

$$\int_0^H \bar{u}\frac{\partial \bar{w}}{\partial x}\,dy=\frac{\partial}{\partial x}\int_0^H \overline{uw}\,dy=\frac{\partial}{\partial x}(\Gamma_{ra}Hu_mw_m) \qquad \int_0^H \frac{\partial \bar{v}}{\partial t}\,dy=\frac{\partial H}{\partial t}$$

For a fully developed turbulent flow regime the velocity profile shape becomes flat, and the quantity is close to unity as shown in Burton's experiments (ref. 11).

$$\Gamma_{rr}=\Gamma_{ar}=\Gamma_{ra}=\Gamma_{aa}=1 \tag{4}$$

Equations (1) to (3) can be rewritten as

$$\frac{\partial (Hu_m)}{\partial t} + \frac{\partial (Hu_m^2)}{\partial x} + \frac{\partial (Hu_m w_m)}{\partial z} = -H\frac{\partial P}{\partial x} + \tau_{tr}\Big|_0^H \tag{5}$$

$$\frac{\partial (Hw_m)}{\partial t} + \frac{\partial (Hu_m w_m)}{\partial x} + \frac{\partial (Hw_m^2)}{\partial z} = -H\frac{\partial P}{\partial z} + \tau_{ta}\Big|_0^H \tag{6}$$

$$\frac{\partial H}{\partial t} + \frac{\partial (Hu_m)}{\partial x} + \frac{\partial (Hw_m)}{\partial z} = 0 \tag{7}$$

Assumptions for Analysis

The assumptions for this analysis are as follows:

(1) The fluid is liquid and incompressible.

(2) The fluid flows into the groove chamber with a constantly diverging angle (ref. 12). This is illustrated in figure 2.

(3) For a small motion of the seal journal about a centered position, the streamline in the groove moves with the journal.

(4) The groove cross section is rectangular.

DERIVATION OF SHEAR STRESS IN MOMENTUM EQUATION

The shear stress terms of equations (4) and (5) are discussed here.

Land. - The axial components τ_{lsa}, τ_{lja} of shear stress at the casing and journal are given by

$$\tau_{lsa} = -\tau_{lja} = \tau_{la} = \frac{1}{2}\rho\lambda_{la}\omega_{lm}^2 \tag{8}$$

where λ_{la} defines the friction coefficient between the flow and the wall surface:

$$\lambda_{la} = 0.0665\left(\frac{\omega_{lm}H_l}{\nu}\right)^{-0.25}\left\{1+\left(\frac{7V}{16\omega_{lm}}\right)^2\right\}^{3/8} \tag{9}$$

The circumferential components τ_{lsr}, τ_{ljr} of shear stress at the casing and journal are given by

$$\tau_{lsr} = \tau_{la}\frac{u_{lm}}{\omega_{lm}} = \frac{1}{2}\rho\lambda_{la}\omega_{lm}u_{lm}$$

$$\tau_{ljr} = \tau_{la}\frac{R\omega - u_{lm}}{\omega_{lm}} = \frac{1}{2}\rho\lambda_{la}\omega_{lm}(R\omega - u_{lm}) \tag{10}$$

This equation is strictly applicable only for $R_a \gg R_r$. Therefore the shear stress of the land can be written as follows:

$$\left.\begin{aligned} \tau_{tr}\Big|_0^H &= \tau_{ljr} - \tau_{lsr} = -\rho\lambda_{la}\omega_{lm}\left(u_{lm} - \frac{1}{2}R\omega\right) \\ \tau_{ta}\Big|_0^H &= \tau_{lja} - \tau_{lsa} = -\frac{12\mu_a\omega_{lm}}{H} \end{aligned}\right\} \tag{11}$$

Where the effective viscosity μ_a (ref. 13) is

$$\mu_a = 0.01(7-3\beta)R_a\lambda_{la}\mu \qquad \beta = \left(\frac{7V}{16\omega_{lm}}\right)\Big/\left\{1+\left(\frac{7V}{16\omega_{lm}}\right)^2\right\}$$

Groove. - The crossflow in the groove is considered to be the cavity flow plus the clearance flow (fig. 2). The exchange of energy within a small mixing area between both flows is influenced by the entrance velocity and the geometric shape of the groove. The clearance flow can be described by a stream tube if this mixing area is replaced by a separating layer. The cavity flow assumes that the momentum that is supplied from the journal is balanced by the sum of the momentum lost by fluid friction at the separating layer and the momentum due to cavity flow. If the cavity flow is replaced with flow through a circular pipe, the fluid mean depth of groove MG is given as

$$MG = \frac{L_g\left|T+(T-L_g\tan\theta)\right|}{2\left(L_g+T+\ T-L_g\tan\theta+L_g/\cos\theta\right)} \tag{12}$$

The friction coefficient between the groove wall and the fluid is

$$\lambda_d = 0.0791\left(\frac{u_{dm}\cdot 4MG}{\nu}\right)^{-0.25} \tag{13}$$

Therefore the momentum that is supplied from the side and root of the groove is expressed, where

$$\frac{1}{2}\rho\lambda_d\left\{\left(R-T+\frac{4MG}{2}\right)\omega-u_{dm}\right\}^2\times\left\{T+(T-L_g\tan\theta)+L_g\right\} \tag{14}$$

And the momentum that is lost from the fluid friction between the clearance flow and the cavity flow is

$$\frac{1}{2}\rho\lambda_f(u_{dm}-u_{gm})^2 \cdot L_g/\cos\theta \tag{15}$$

where λ_f defines the fluid friction loss coefficient between the cavity flow and clearance flow, and $\lambda_f = 0.1$ (ref. 14). Using equations (14) and (15), one can calculate the circumferential fluid velocity of the cavity flow U_{dm}. The axial component of shear stress is given by

$$\tau_{gsa} = \frac{1}{2}\rho\lambda_{ga}\omega_{gm}^2, \quad \tau_{gfa} = \frac{1}{2}\rho\lambda_f(\omega_{gm}-\omega_{dm})^2 = \frac{1}{2}\rho\lambda_f(\omega_{gm}-0.5\omega_{gm})^2 \tag{16}$$

and the circumferential component by

$$\left.\begin{aligned} \tau_{gsr} &= \tau_{gsa}\frac{u_{gm}}{\omega_{gm}} = \frac{1}{2}\rho\lambda_{ga}\omega_{gm}u_{gm} \\ \tau_{gfr} &= \tau_{gfa}\frac{u_{dm}-u_{gm}}{\omega_{gm}} = \frac{1}{8}\rho\lambda_f\omega_{gm}(u_{dm}-u_{gm}) \end{aligned}\right\} \tag{17}$$

where

$$\lambda_{ga} = 0.0665\left(\frac{\omega_{gm}H_g}{\nu}\right)^{-0.25}\left\{1+\left(\frac{7u_{dm}}{16\omega_{gm}}\right)^2\right\}^{3/8}$$

Therefore the shear stress of the groove can be written as

$$\left.\begin{aligned} \tau_{tr}\Big|_0^H &= \tau_{gfr}-\tau_{gsr} = \frac{1}{2}\rho 0.25\lambda_f\omega_{gm}(u_{dm}-u_{gm}) - \frac{1}{2}\rho\lambda_{ga}\omega_{gm}u_{gm} \\ \tau_{ta}\Big|_0^H &= \tau_{gfa}-\tau_{gsa} = -\frac{1}{2}\rho(\lambda_{ga}+0.25\lambda_f)\omega_{gm}^2 \end{aligned}\right\} \tag{18}$$

Derivation of Static Characteristics

Axial fluid velocity. - The pressure loss is stated as follows: The inlet loss at the land entrance is

$$\Delta P_{lin} = \frac{1}{2}\rho\xi_1\omega_{lo}^2 \tag{19}$$

where

$$\xi_1 = 1.5 \qquad \text{(at 1st stage)}$$

$$\xi_1 = 1+0.824\delta_2-(1+0.824\delta_1)\left(\frac{H_2}{H_1}\right)^2 \quad \text{(after 2nd stage)}$$

$$\delta_1 = 1.95\left(\frac{\omega_{lo} H_1}{\nu}\right)^{-0.43} \qquad \delta_2 = 1.95\left(\frac{\omega_{lo} H_2}{\nu}\right)^{-0.43}$$

$$H_1 = C_{lo}+L_g\tan\theta \qquad H_2 = C_{lo}$$

The wall friction loss in the land is

$$\Delta P_l = 2\frac{L_{lo}}{C_{lo}}\cdot\frac{1}{2}\rho\lambda_{la}\omega_{lo}^2 \tag{20}$$

The exit loss due to diverging flow behind the land is

$$\Delta P_{lex} = \frac{1}{2}\rho\xi_2\omega_{lo}^2 \tag{21}$$

where ξ_2 is the exit loss coefficient

$$\xi_2 = \left(1-\frac{C_{lo}}{C_{lo}+L_g\tan\theta}\right)^2 \quad \text{(at each stage)}$$

$$\xi_2 = \left(1-\frac{C_{lo}}{C_{lo}+T}\right)^2 \quad \text{(at seal exit)}$$

The friction loss at the wall and the separating layer of the groove is

$$\Delta P_g = \frac{1}{2}\rho\omega_{lo}^2(\lambda_{ga}+0.25\lambda_f)\left(\frac{C_{lo}}{C_{lo}+L_g/2\cdot\tan\theta}\right)^2\frac{L_g}{C_{lo}+L_g\tan\theta} \tag{22}$$

The pressure restoration due to deceleration at the groove is

$$\Delta P_{gup} = \frac{2C_{lo}}{C_{lo}+L_g\tan\theta}\left(1-\frac{C_{lo}}{C_{lo}+L_g\tan\theta}\right)\frac{1}{2}\rho\omega_{lo}^2 \tag{23}$$

The pressure drop across the seal is equal to the sum of each pressure loss and is stated as follows:

$$P_{in}-P_{ex} = \Delta P'_{lin} + S(\Delta P_l + \Delta P_{lex} + \Delta P_g - \Delta P_{gup} + \Delta P_{lin}) + \Delta P_l + \Delta P'_{lex}$$

$$= \frac{1}{2}\rho\xi'_1\omega^2_{lo} + S\left[\frac{1}{2}\rho\omega^2_{lo}\frac{2L_l}{C_{lo}}\lambda_{la} + \frac{1}{2}\rho\omega^2_{lo}\left(1-\frac{C_{lo}}{C_{lo}+L_g\tan\theta}\right)^2\right.$$

$$+\frac{1}{2}\rho\omega^2_{lo}(\lambda_{ga}+0.25\lambda_f)\left(\frac{C_{lo}}{C_{lo}+L_g/2\ \tan\theta}\right)^2\frac{L_g}{C_{lo}+L_g/2\cdot\tan\theta}$$

$$-\frac{1}{2}\rho\omega^2_{lo}\frac{2C_{lo}}{C_{lo}+L_g\tan\theta}\left(1-\frac{C_{lo}}{C_{lo}+L_g\tan\theta}\right)$$

$$\left.+\frac{1}{2}\rho\omega^2_{lo}\ \xi_1\right]$$

$$+\frac{1}{2}\rho\omega^2_{lo}\frac{2L_l}{C_{lo}}\lambda_{la} + \frac{1}{2}\rho\omega^2_{lo}\left(1-\frac{C_{lo}}{C_{lo}+L_g\tan\theta}\right)^2 \qquad (24)$$

Rate of leakage. - The main advantage of the grooved seal is that leakage flow can be minimized but seal components need never rub. Seal leakage flow may also be denoted by Q, where

$$Q = \int_R^{R+T} w_{lo}\ 2\pi r\ dr = \pi w_{lo}C_{lo}(2R+C_{lo}) \qquad (25)$$

Figure 3 shows the calculated results of leakage flow. As the number of stages increased or the land became narrower, the leakage flow decreased.

Circumferential fluid velocity. - From the momentum equation (5) for the land

$$\frac{\partial u_{lo}}{\partial z} + \frac{1}{l}u_{lo} = \frac{1}{l}\cdot\frac{V}{2} \qquad (26)$$

where $l = C_{lo}/\lambda_a$ and $V = R\omega$. The boundary condition is $z = z_{n-1/2}$; $u_{lo} = u_{lo(z_{n-1/2})}$. The circumferential fluid velocity u_{lo} at the land is

$$u_{lo} = \frac{V}{2} - \left\{\frac{V}{2} - u_{lo(z_{n-\frac{1}{2}})}\right\}\cdot e^{-z/l} \qquad (27)$$

From the momentum equation (5) for the groove

$$\frac{\partial u_{go}}{\partial z} + \frac{u_{go}}{2C_{go}}(\lambda_{ga}+0.25\lambda_f) = \frac{\lambda_f u_{dm}}{8C_{go}} \qquad (28)$$

where u_{dm} can be calculated from equations (14) and (15) and the boundary condition is

$$z = z_n \qquad u_{go} = u_{go(z_n)}$$

The circumferential fluid velocity u_{go} at the groove is

$$u_{go} = u_z - u_{ug} C_{go}^{-A/\tan\theta} \tag{29}$$

where

$$u_{ug} = u_z - u_{go(z_n)} \qquad A = \lambda_{ga} + 0.25\lambda_f \qquad u_z = \frac{\lambda_f u_{dm}}{\theta A}$$

Figure 4 shows the axial distribution of circumferential fluid velocity ΔP = 0.49 MPa, N = 4000 rpm, L = 55 mm, and S = 20. The results indicate that the circumferential velocity approaches one-half of the shaft angular velocity exponentially.

Torque loss. - The method for estimating the torque loss in a grooved seal treats the loss as frictional dissipation by viscous shear in an annulus. From equation (10) the torque loss of the land is

$$Torq_l = \int_0^{2\pi}\int_0^{L_l} \tau_{ljr} \times R \times R\,d\phi\,dz$$

$$= \rho\pi R^2 \lambda_{la} w_{lo} \left(\frac{V}{2} L_l + \left\{\frac{V}{2} - u_{lo(z_{n-1/2})}\right\} \cdot l\left(e^{-L_l/l} - 1\right)\right) \tag{30}$$

The torque loss of the groove assumes that the groove is divided into four parts as shown in figure 5. The shear stress of part 1 is

$$\tau_{g1} = \frac{1}{2}\rho\lambda_d u_{dm}^2 \tag{31}$$

Therefore the torque loss of part 1 is given as follows:

$$\tau_{g1} = \int_0^{2\pi}\int_{R-T}^{R} \tau_{g1} \times r \times r\,d\phi\,dr = \frac{2\pi}{3}\left\{R^3 - (R-T)^3\right\} \cdot \frac{1}{2}\rho\lambda_d u_{dm}^2$$

Similarly

$$\tau_{g2} = \int_0^{2\pi}\int_0^{L_g} \tau_{g2} \times (R-T) \times (R-T)\,d\phi\,dz = \rho\pi(R-T)^2 L_g \lambda_d u_{dm}^2$$

$$T_{g3} = \int_0^{2\pi}\int_{R-T}^{R-L_g \tan\theta} \tau_{g3} \times r \times r\,d\phi\,dr = \frac{2\pi}{3}\left\{(R-L_g\tan\theta)^3-(R-T)^3\right\}\frac{1}{2}\rho\lambda_d u_{dm}^2$$

$$T_{g4} = \int_0^{2\pi}\int_{R-L_g\tan\theta}^{R} \tau_{g4} \times r \times r\,d\phi\,dr$$

$$= \frac{2\pi}{3}\left\{R^3-(R-L_g\tan\theta)^3\right\}\frac{1}{2}\rho\lambda_{ga}\frac{C_{lo}\omega_{lo}}{C_{lo}+L_g\tan\theta}u_{go(z_{n+1/2})}$$

Therefore the torque loss of the groove is

$$Torq_g = T_{g1} + T_{g2} + T_{g3} + T_{g4} \tag{32}$$

And the total torque loss of the parallel-grooved seal is defined by the following equation:

$$\Delta T = \sum_{i=1}^{S+1} Torq_l + \sum_{i=1}^{S} Torq_g \tag{33}$$

Figure 6 shows the torque loss of the parallel-grooved seal for ΔP = 0.49 MPa and L = 55 mm without inlet swirl. As the number of stages increased or the seal clearance decreased, the torque loss increased.

Derivation of Pressure Distribution

For a small motion about a centered position the clearance, pressure, and velocity are expanded in the perturbation variables as follows:

$$H = C_o + \varepsilon\psi \qquad P = P_o + \varepsilon P_1 \qquad \omega_m = \omega_o + \varepsilon\omega_1 \qquad u_m = u_o + \varepsilon u_1 \tag{34}$$

where C_0, P_0, ω_0, u_0 are steady-state values and ψ, P_1, w_1, u_1 are small perturbations. The short-bearing solution (ref. 4) is developed for the first-order equation by neglecting u_1, the pressure-induced circumferential velocity component.

Static pressure distribution. - The steady-state equation described is static, has zero eccentricity, and is solved analytically. Substitution of equation (6) into equations (11), (18), and (34) yields steady-state, axial-direction momentum equations for the land

$$\frac{\partial P_{lo}}{\partial z} = -\frac{12\mu_a\omega_{lo}}{C_{lo}^2} \tag{35}$$

and for the groove

$$\frac{\partial P_{go}}{\partial z} = -\frac{\rho C_{lo}^2 \omega_{lo}^2 \lambda_{sa}}{2(C_{lo}+z\tan\theta)^2} \tag{36}$$

where λ_{sa} defines the equivalent friction coefficient of the groove.

$$\lambda_{sa} = \lambda_{ga} + 0.25\lambda_f - 2\tan\theta$$

Pressure distribution of nonsteady state. - Substitution of the perturbation variables of equations (6) and (7) yields the following perturbation equation for the land:

$$\frac{\partial P_{l1}}{\partial z} = -\frac{\psi}{C_{lo}} \cdot \frac{\partial P_{lo}}{\partial z} - \frac{12\mu_a \omega_{l1}}{C_{lo}^2}$$
$$-\rho\left(\frac{\partial \omega_{l1}}{\partial t} + \frac{\omega_{lo}}{C_{lo}} \cdot \frac{\partial \psi}{\partial t} + u_{lo}\frac{\partial \omega_{l1}}{\partial x} + \frac{u_{lo}\omega_{lo}}{C_{lo}} \cdot \frac{\partial \psi}{\partial x} + 8\omega_{lo}\frac{\partial \omega_{l1}}{\partial z}\right) \tag{37}$$

$$\frac{\partial \omega_{l1}}{\partial z} = -\frac{1}{C_{lo}}\left(\frac{\partial \psi}{\partial t} + u_{lo}\frac{\partial \psi}{\partial x}\right) \tag{38}$$

Equation (38) can be integrated by using the boundary condition $z = z_{n-1/2}$, $w_{l1} = w_{l1}(z_{n-1/2})$ as follows:

$$\omega_{l1} = \omega_{l1(z_{n-1/2})} - \frac{1}{C_{lo}} f_l(x,t)(z - z_{n-1/2}) - \frac{l}{C_{lo}} u_{ul} \frac{\partial \psi}{\partial x}(e^{-z/l} - 1) \tag{39}$$

where

$$f_l(x,t) = \frac{\partial \psi}{\partial t} + \frac{V}{2} \cdot \frac{\partial \psi}{\partial x} \qquad u_{ul} = \frac{V}{2} - u_{lo(z_{n-1/2})}$$

Equation (19) yields the following perturbation-variable boundary condition at the seal inlet:

$$P_{l1(z_{n-1/2})} = -\rho\xi_1 \omega_{lo}\omega_{l1(z_{n-1/2})} \tag{40}$$

The perturbation-variable boundary condition at the seal exit is given as

$$z = z_n \; ; \; P_{l1(z_n)} = 0 \tag{41}$$

The complete solution for the perturbation pressure is obtained as

$$P_{l1} = \frac{12\mu_a \omega_{lo}\psi}{C_{lo}^3} PRL1 + \frac{6\mu_a}{C_{lo}^3} f_l(x,t) \cdot PRL2$$

$$-\frac{12\mu_a u_{ul}{}^l}{C_{lo}^2} \cdot \frac{\partial\psi}{\partial x} PRL6 + \frac{\rho}{2C_{lo}}\left(\frac{\partial}{\partial t} + \frac{V}{2}\cdot\frac{\partial}{\partial x}\right) f_l(x,t)\ PRL2$$

$$-\frac{\rho u_{ul}{}^l}{C_{lo}}\left(\frac{\partial}{\partial t} + \frac{V}{2}\cdot\frac{\partial}{\partial x}\right)\left(\frac{\partial\psi}{\partial x}\right) PRL6 + \frac{\rho u_{ul}{}^l}{C_{lo}} \cdot \frac{\partial}{\partial x} f_l(x,t)\ PRL7$$

$$-\frac{\rho u_{ul}^2 l^2}{C_{lo}} \frac{\partial}{\partial x}\left(\frac{\partial\psi}{\partial x}\right) PRL8 + \frac{\rho\omega_{lo}}{C_{lo}} f_l(x,t)\ PRL1 + \frac{\rho\omega_{lo}u_{ul}{}^l}{C_{lo}} \cdot \frac{\partial\psi}{\partial x} PRL2 \qquad (42)$$

where PRL1 to PRL8 are provided in appendix A.

Similarly for the groove the axial-momentum equation and the continuity equation reduce to

$$\frac{\partial P_{g1}}{\partial z} = -\frac{\psi}{C_{go}} \cdot \frac{\partial P_{go}}{\partial z} - \frac{\rho}{C_{go}}(\lambda_{ga} + 0.85\lambda_f)\omega_{go}\omega_{g1}$$

$$-\rho\left(\frac{\psi\omega_{go}}{C_{go}} \cdot \frac{\partial\omega_{go}}{\partial z} + \frac{\partial\omega_{g1}}{\partial t} + u_{go}\frac{\partial\omega_{g1}}{\partial x} + \omega_{go}\frac{\partial\omega_{g1}}{\partial z} + \omega_{g1}\frac{\partial\omega_{go}}{\partial z}\right) \qquad (43)$$

$$u_{go}\frac{\partial\psi}{\partial x} + \psi\frac{\partial\omega_{go}}{\partial z} + C_{go}\frac{\partial\omega_{g1}}{\partial z} + \omega_{g1}\frac{\partial C_{go}}{\partial z} + \frac{\partial\psi}{\partial t} = 0 \qquad (44)$$

Substitution of equation (29) and the boundary condition $z = z_n$, $w_{g1} = w_{g1}(z_n)$ into equation (44) yields

$$\omega_{g1} = \omega_{g1(z_n)}\frac{C_{lo}}{C_{go}} - f_g(x,t)\frac{z - z_n}{C_{go}}$$

$$-\frac{u_{ug}}{A - \tan\theta} \cdot \frac{C_{go}^{-a+1} - C_{lo}^{-a+1}}{C_{go}} \cdot \frac{\partial\psi}{\partial x} + \frac{\psi\omega_{lo}(z - z_n)\tan\theta}{C_{go}^2} \qquad (45)$$

where

$$f_g(x,t) = \frac{\partial\psi}{\partial t} + u_z \cdot \frac{\partial\psi}{\partial x} \qquad a = A/\tan\theta$$

The pressure boundary condition is

$$z = z_n \qquad P_{g1} = P_{g1(z_n)} \qquad (46)$$

The perturbation-variable boundary condition is obtained as

$$P_{g1(z_n)} = -\rho\xi_2\omega_{lo}\omega_{g1(z_n)} \tag{47}$$

The complete solution for the perturbation pressure is obtained as

$$\begin{aligned}
P_{g1} = {} & -\frac{\rho C_{lo}^2\omega_{lo}^2\lambda_{sa}\psi}{6\tan\theta}\cdot PRG1 + \rho C_{lo}\omega_{lo}\lambda_{sa}\cdot f_g(x,t)\cdot PRG14 + \frac{\rho C_{lo}\omega_{lo}u_{ug}}{A+\tan\theta}\cdot\frac{\partial\psi}{\partial x}\cdot PRG6 \\
& -\frac{\rho u_{ug}\omega_{lo}\tan\theta}{A+\tan\theta}\cdot\frac{\partial\psi}{\partial x}\,PRG18 - \frac{\rho C_{lo}\omega_{lo}}{\tan\theta}\cdot f_g(x,t)\cdot PRG2 + \frac{\rho u_{ug}}{A-\tan\theta}\cdot\frac{\partial}{\partial x}\left(\frac{\partial\psi}{\partial x}\right)PRG21 \\
& +\rho\left(\frac{\partial}{\partial t}+u_z\cdot\frac{\partial}{\partial x}\right)f_g(x,t)\cdot PRG16 + \frac{\rho C_{lo}\omega_{lo}u_{ug}\lambda_{sa}}{A-\tan\theta}\cdot\frac{\partial\psi}{\partial x}\cdot PRG19 \\
& -\rho C_{lo}\omega_{lo}^2\tan\theta\lambda_{sa}\cdot PRG13 - \frac{\rho u_{ug}}{A-\tan\theta}\left(\frac{\partial}{\partial t}+u_z\cdot\frac{\partial}{\partial x}\right)\left(\frac{\partial\psi}{\partial x}\right)PRG17 \\
& +\frac{\rho u_{ug}}{A}\cdot\frac{\partial}{\partial x}f_g(x,t)\cdot PRG20 - \rho\omega_{lo}\tan\theta\, f_g(x,t)\cdot PRG15
\end{aligned} \tag{48}$$

where PRG1 to PRG2 are provided in appendix B.

Dynamic Force

For a small motion about a centered position the clearance function is defined in terms of the radial seal displacement ($\Delta X, \Delta Y$).

$$\varepsilon\psi = -\Delta X\cos\phi - \Delta Y\sin\phi \tag{49}$$

The components of the reaction force acting on the seal journal are defined by the integrals

$$\left.\begin{aligned}
F_X &= -\left[\sum_{n=1}^{S}\int_0^{2\pi}\left\{\int_{z_{n-1/2}}^{z_n}\varepsilon P_{l1} + \int_{z_n}^{z_{n+1/2}}\varepsilon P_{g1}\right\} + \int_0^{2\pi}\int_{z_{S+1/2}}^{z_{S+1}}\varepsilon P_{l1}\right]\cos\phi R d\phi dz \\
F_Y &= -\left[\sum_{n=1}^{S}\int_0^{2\pi}\left\{\int_{z_{n-1/2}}^{z_n}\varepsilon P_{l1} + \int_{z_n}^{z_{n+1/2}}\varepsilon P_{g1}\right\} + \int_0^{2\pi}\int_{z_{S+1/2}}^{z_{S+1}}\varepsilon P_{l1}\right]\sin\phi R d\phi dz
\end{aligned}\right\} \tag{50}$$

Substituting for ψ and its derivatives into equations (42) and (48) yields the following form for the seal coefficients:

$$-\begin{bmatrix}F_X\\F_Y\end{bmatrix} = \begin{bmatrix}K_{XX} & K_{XY}\\K_{YX} & K_{YY}\end{bmatrix}\begin{bmatrix}X\\Y\end{bmatrix} + \begin{bmatrix}C_{XX} & C_{XY}\\C_{YX} & C_{YY}\end{bmatrix}\begin{bmatrix}\dot{X}\\\dot{Y}\end{bmatrix} + \begin{bmatrix}M_{XX} & M_{XY}\\M_{YX} & M_{YY}\end{bmatrix}\begin{bmatrix}\ddot{X}\\\ddot{Y}\end{bmatrix} \tag{51}$$

Because the seal coefficients of each stage are different, the following definitions are used. The dynamic coefficients of the parallel-grooved seal become

$$\left.\begin{aligned} K_{XX} &= \sum_{n=1}^{S+1} K_{XXl} + \sum_{n=1}^{S} K_{XXg} & K_{YX} &= \sum_{n=1}^{S+1} K_{YXl} + \sum_{n=1}^{S} K_{YXg} \\ C_{XX} &= \sum_{n=1}^{S+1} C_{XXl} + \sum_{n=1}^{S} C_{XXg} & C_{YX} &= \sum_{n=1}^{S+1} C_{YXl} + \sum_{n=1}^{S} C_{YXg} \\ M_{XX} &= \sum_{n=1}^{S+1} M_{XXl} + \sum_{n=1}^{S} M_{XXg} & M_{YX} &= \sum_{n=1}^{S+1} M_{YXl} + \sum_{n=1}^{S} M_{YXg} = 0 \end{aligned}\right\} \quad (52)$$

where

$$K_{XX} = K_{YY} \qquad K_{YX} = -K_{XY} \qquad C_{XX} = C_{YY}$$

$$C_{YX} = -C_{XY} \qquad M_{XX} = M_{YY} \qquad M_{YX} = -M_{XY} = 0$$

The dynamic seal coefficients for the land are

$$K_{XXl} = -\frac{\pi R}{C_{lo}}\left[\frac{12\mu_a \omega_{lo}}{C_{lo}^2} IPRL1 - \frac{\rho V^2}{8R^2} IPRL2 + \frac{\rho u_{ul} l V}{2R^2}(IPRL4 - IPRL7) + \frac{\rho u_{ul}^2 l^2}{R^2} IPRL8\right] = K_{YYl}$$

$$K_{YXl} = \frac{\pi}{C_{lo}}\left[\frac{6\mu_a}{C_{lo}^2}\frac{V}{2} IPRL2 - \frac{12\mu_a u_{ul} l}{C_{lo}^2} IPRL4 + \frac{\rho\omega_{lo} V}{2} IPRL1 + \rho\omega_{lo} u_{ul} l\ IPRL3\right] = -K_{XYl}$$

$$C_{XXl} = -\frac{\pi R}{C_{lo}}\left[\frac{6\mu_a}{C_{lo}^2} IPRL2 + \rho\omega_{lo} IPRL1\right] = C_{YY}$$

$$C_{YX1} = \frac{V}{C_{lo}} \frac{V}{2} IPRL2 - u_{ul}{}^{l}\ IPRL4 + u_{ul}{}^{l}\ IPRL7 = -C_{XY1}$$

$$C_{YX1} = \frac{\rho\pi}{C_{lo}}\left[\frac{V}{2} IPRL2 - u_{ul}{}^{l}(IPRL4-IPRL7)\right] = -C_{XY1}$$

$$M_{XX1} = -\frac{\rho\pi R}{2C_{lo}} \cdot IPRL2 = M_{YY1} \qquad M_{YX1} = M_{XY1} = 0$$

where IPRL1 to IPRL8 are provided in appendix C. The dynamic seal coefficients for the groove are

$$K_{XXg} = \rho\pi R\left[\frac{C_{lo}^2 \omega_{lo}^2 \lambda_{sa}}{6\tan\theta} IPRG1 + C_{lo}\omega_{lo}^2 \tan\theta\lambda_{sa} \cdot IPRG13\right.$$

$$+\frac{u_z^2}{R^2} IPRG16 - \frac{u_{ul}u_z}{(A-\tan\theta)R^2} \cdot IPRG17$$

$$\left.+\frac{u_{ul}u_z}{A\ R^2} IPRG20 + \frac{u_{ul}^2}{(A-\tan\theta)R^2} IPRG21\right] = K_{YYg}$$

$$K_{YXg} = \rho\pi C_{lo}\omega_{lo}\left[u_z\lambda_{sa}\ IPRG14 + \frac{u_{ul}\lambda_{sa}}{A-\tan\theta} IPRG19\right.$$

$$-\frac{u_z\tan\theta}{C_{lo}} IPRG15 - \frac{u_{ul}\tan\theta}{C_{lo}(A+\tan\theta)} \cdot IPRG18$$

$$\left.-\frac{u_z}{\tan\theta} IPRG2 + \frac{u_{ul}}{A+\tan\theta} IPRG4\right] = -K_{XYg}$$

$$C_{XXg} = \rho\pi RC_{lo}\omega_{lo}\left[-\lambda_{sa}\ IPRG14 + \frac{\tan\theta}{C_{lo}}\ IPRG15 + \frac{1}{\tan\theta}\ IPRG2\right] = C_{YYg}$$

$$C_{YXg} = \rho\pi\left[2u_z\ IPRG16 - \frac{u_{ul}}{A-\tan\theta}\ IPRG17 + \frac{u_{ul}}{A}\ IPRG20\right] = -C_{XYg}$$

$$M_{XXg} = -\rho\pi R \cdot IPRG16 = M_{YYg}$$

$$M_{YXg} = M_{XYg} = 0$$

where IPRG1 to IPRG21 are provided in appendix C.

NUMERICAL EXAMPLE

Seal coefficients were calculated for a pump seal with the characteristics shown in table I. The dynamic coefficients decreased with an increase in the number of stages (fig. 7); that is, the axial Reynolds number became small because the pressure loss increased with an increase in the number of stages. The cross-coupling terms were relatively sensitive to swirl at the seal entrance; as the inlet swirl was propagated right through, the mean circumferential fluid velocity approaches one-half the journal speed exponentially (ref. 15).

Figure 8 illustrates the influence of the ratio L_{lg} of land width L_l to groove width plus land width ($L_l + L_g$) for $N = 4000$ rpm and $L/D = 0.25$. As the clearance ratio C_l/C_g became small, the dynamic coefficients became large with an increase in the ratio L_{lg}.

CONCLUSIONS

The static and dynamic characteristics of the annular parallel-grooved seal were theoretically investigated with consideration for the effect of the turbulent flow and the inertia term.

As the number of stages increases or the land becomes narrower, the dynamic coefficients and the leakage flow rate decrease. But torque loss increases rapidly.

APPENDIX A

$$q_{l1} = \rho\omega_{lo}\left\{1+0.824\delta_2 -(1+0.824\delta_1)\left(\frac{H_2}{H_1}\right)^2\right\} + \frac{12\mu_a L_l}{C_{lo}^2}$$

$$q_{l2} = \rho\omega_{lo}\left\{1+0.824\delta_2 -(1+0.824\delta_1)\left(\frac{H_2}{H_1}\right)^2\right\}$$

$$m = \frac{1}{q_{l1}}\left(q_{l2} + \frac{12\mu_a}{C_{lo}}(z - z_{n-1/2})\right)$$

$$PRL1 = z - z_{n-1/2} - m\,L_l$$

$$PRL2 = (z - z_{n-1/2})^2 - m\cdot L_l^2$$

$$PRL3 = e^{-z/l} - 1 - m\cdot(e^{-L_l/l} - 1)$$

$$PRL4 = e^{-2z/l} - 1 - m\cdot(e^{-2L_l/l} - 1)$$

$$PRL5 = (z - z_{n-1/2})\cdot e^{-z/l} - m\,L_l\cdot e^{-L_l/l}$$

$$PRL6 = PRL1 + l\,PRL3$$

$$PRL7 = l\cdot PRL3 + PRL5$$

$$PRL8 = PRL3 - \frac{1}{2}PRL4$$

APPENDIX B

$$q_{g1} = \rho\omega_{lo}\left\{\left(1-\frac{C_{lo}}{C_1}\right)^2 - \frac{C_{lo}\lambda_{sa}}{2\tan\theta}\left(\frac{1}{C_1^2} - \frac{1}{C_{lo}^2}\right)\right\}$$

$$q_{g2} = \rho\omega_{lo}\left\{\left(1-\frac{C_{lo}}{C1}\right)^2 + \frac{\lambda_{sa}}{2\tan\theta}\right\}$$

$$m = \frac{1}{q_{g1}}\left\{q_{g2} - \frac{\rho\omega_{lo}C_{lo}\lambda_{sa}}{2\tan\theta}\cdot\frac{1}{C_{go}}\right\}$$

$$J1 = 1/C_1 - 1/C_{lo} \qquad J2 = 1/C_1^2 - 1/C_{lo}^2$$

$$J3 = 1/C_1^3 - 1/C_{lo}^3 \qquad J4 = \ln(C_1/C_{lo})$$

$$J5 = C_1^{-a-1} - C_{lo}^{-a-1} \qquad J6 = C_1^{-a+2} - C_{lo}^{-a+2}$$

$$J7 = C_1^{-a+1} - C_{lo}^{-a+1} \qquad J8 = C_1^{-a} - C_{lo}^{-a}$$

$$J9 = C_1^{-2a+1} - C_{lo}^{-2a+1}$$

$$J10 = \frac{1}{q_{g1}}\,\rho\omega_{lo}\left\{\left(1-\frac{C_{lo}}{C_{go}}\right)^2 + \frac{\lambda_{sa}}{2\tan\theta}\right\}$$

$$J11 = \frac{1}{q_{g1}}\cdot\frac{\rho C_{lo}\omega_{lo}\lambda_{sa}}{2\tan\theta}$$

$$J12 = (J10\cdot L_g + J11\cdot J1)$$

$$J13 = C_1^{-a+3} - C_{go}^{-a+3}$$

$$J14 = C_1^{-2a+2} - C_{go}^{-2a+2}$$

$$PRG1 = \frac{1}{C_{go}^3} - \frac{1}{C_{lo}^3} - m \cdot J3 \qquad PRG2 = \frac{1}{C_{go}} - \frac{1}{C_{lo}} - m \cdot J1$$

$$PRG3 = \frac{1}{C_{go}^2} - \frac{1}{C_{lo}^2} - m \cdot J2 \qquad PRG4 = \ln(C_{go}/C_{lo}) - m \cdot J4$$

$$PRG5 = z - z_n - m \cdot L_g \qquad PRG6 = C_{go}^{-a-1} - C_{lo}^{-a-1} - m \cdot J5$$

$$PRG7 = C_{go}^{-a+2} - C_{lo}^{-a+2} - m \cdot J6$$

$$PRG8 = (z - z_n)\, C_{go}^{-a-1} - m\, L_g \cdot C_1^{-a-1}$$

$$PRG9 = C_{go}^{-a+1} - C_{lo}^{-a+1} - m \cdot J7 \qquad PRG10 = C_{go}^{-a} - C_{lo}^{-a} - m \cdot J8$$

$$PRG11 = (z - z_n)\, C_{go}^{-a} - m\, L_g \cdot C_1^{-a}$$

$$PRG12 = C_{go}^{-2a+1} - C_{lo}^{-2a+1} - m \cdot J9$$

$$PRG13 = \frac{1}{\tan^2\theta}\left(\frac{C_{lo}}{3}\, PRG1 - \frac{1}{2}\, PRG3\right)$$

$$PRG14 = \frac{1}{\tan^2\theta}\left(-\, PRG2 + \frac{C_{lo}}{2}\, PRG3\right)$$

$$PRG15 = \frac{1}{\tan^2\theta}\left(C_{lo}\, PRG2 + PRG4\right)$$

$$PRG16 = \frac{1}{\tan^2\theta}\left(-C_{lo}\, PRG4 + \tan\theta \cdot PRG5\right)$$

$$PRG17 = \frac{1}{A - \tan\theta}\, PRG9 + \frac{C_{lo}^{-a+1}}{\tan\theta}\, PRG4$$

$$PRG18 = PRG8 + \frac{1}{A}\, PRG10$$

$$PRG19 = -\frac{1}{A+\tan\theta}\,PRG6 + \frac{C_{lo}^{-a+1}}{2\tan\theta}\,PRG3$$

$$PRG20 = PRG11 + \frac{1}{A-\tan\theta}\,PRG9$$

$$PRG21 = \frac{1}{2A-\tan\theta}\,PRG12 - \frac{C_{lo}^{-a+1}}{A}\,PRG10$$

APPENDIX C

$$I1 = \frac{1}{q_{l1}}\left(q_{l2}\,L_l + \frac{6\mu_a L_l}{C_{lo}^2}\right)$$

$$IPRL1 = L_l^2/2 - L_l \cdot I1 \qquad IPRL2 = L_l^3/3 - L_l^2/2 \cdot I1$$

$$IPRL3 = -l\left(e^{-L_l/l} - 1\right) - L_l - \left(e^{-L_l/l} - 1\right) \cdot I1$$

$$IPRL4 = l\ IPRL3 + IPRL1$$

$$IPRL5 = -l \cdot L_l e^{-L_l/l} - l^2\left(e^{-L_l/l} - 1\right) - L_l e^{-L_l/l} \cdot I1$$

$$IPRL6 = -\frac{l}{2}\left(e^{-2L_l/l} - 1\right) - L_l - \left(e^{-2L_l/l} - 1\right) \cdot I1$$

$$IPRL7 = l \cdot IPRL3 + IPRL5 \qquad IPRL8 = IPRL3 - \frac{1}{2}\,IPRL6$$

$$C_l = C_{lo} + L_g \tan\theta \qquad IPRG1 = -\frac{J2}{2\tan\theta} - \frac{L_g}{C_{lo}^3} - J3 \cdot J12$$

$$IPRG2 = \frac{J4}{\tan\theta} - \frac{L_g}{C_{lo}} - J1 \cdot J12$$

$$IPRG3 = -\frac{J1}{\tan\theta} - \frac{L_g}{C_{lo}^2} - J2 \cdot J12$$

$$IPRG4 = \frac{C_1}{\tan\theta} J4 - L_g - J4 \cdot J12$$

$$IPRG5 = \frac{L_g^2}{2} - L_g \cdot J12$$

$$IPRG6 = -\frac{J8}{A} - L_g C_{lo}^{-a-1} - J5 \cdot J12$$

$$IPRG7 = -\frac{J13}{A-3\tan\theta} - L_g C_{lo}^{-a+2} - J6 \cdot J12$$

$$IPRG8 = -\frac{L_g}{A} C_1^{-a} - \frac{J7}{A(A-\tan\theta)} - L_g C_1^{-a-1} \cdot J12$$

$$IPRG9 = -\frac{J6}{A-2\tan\theta} - L_g C_{lo}^{-a+1} - J8 \cdot J12$$

$$IPRG10 = -\frac{J7}{A-\tan\theta} - L_g C_{lo}^{-a} - J8 \cdot J12$$

$$IPRG11 = -\frac{L_g C_1^{-a+1}}{A-\tan\theta} - \frac{J6}{(A-\tan\theta)(A-2\tan\theta)} - L_g C_1^{-a} \cdot J12$$

$$IPRG12 = -\frac{J14}{2(A-\tan\theta)} - L_g C_{lo}^{-2a+1} - J9 \cdot J12$$

$$IPRG13 = \frac{1}{\tan^2\theta}\left(\frac{C_{lo}}{3} IPRG1 - \frac{1}{2} IPRG3\right)$$

$$IPRG14 = \frac{1}{\tan^2\theta}\left(-IPRG2 + \frac{C_{lo}}{2} IPRG3\right)$$

$$IPRG15 = \frac{1}{\tan^2\theta}\left(C_{lo} IPRG2 + IPRG4\right)$$

$$IPRG16 = \frac{1}{\tan^2\theta}\left(-C_{lo} IPRG4 + \tan\theta \cdot IPRG5\right)$$

$$IPRG17 = \frac{1}{A-\tan\theta} \cdot IPRG9 + \frac{C_{lo}^{-a+1}}{2\tan\theta} \cdot IPRG4$$

$$IPRG18 = IPRG8 + \frac{1}{A} IPRG10$$

$$IPRG19 = -\frac{1}{A+\tan\theta} IPRG6 + \frac{C_{lo}^{-a+1}}{2\tan\theta} \cdot IPRG3$$

$$IPRG20 = \frac{1}{A-\tan\theta} IPRG9 + IPRG11$$

$$IPRG21 = \frac{1}{2A-\tan\theta} \cdot IPRG12 - \frac{C_{lo}^{-a+1}}{A} \cdot IPRG10$$

REFERENCES

1. Black, H.F.: Effects of Hydraulic Forces in Annular Pressure Seals on the Vibration of Centrifugal Pump Rotors. J. Mech. Eng. Sci., vol. 11, no. 2, 1969, pp. 206-213.

2. Black, H.F.; and Jenssen, D.N.: Dynamic Hybrid Properties of Annular Pressure Seals. Proc. J. Mech. Eng., vol. 184, 1970, pp. 92-100.

3. Black, H.F.; and Jenssen, D.N.: Effects of High-Pressure Ring Seals on Pump Rotor Vibration. ASME Paper 71-WA/FF-38, 1971.

4. Child, D.W.: Dynamic Analysis of Turbulent Annular Seals Based on Hir's Lubrication Equation. J. Lubr. Technol., vol. 105, no. 3, 1983, pp. 429-436.

5. Child, D.W.: Finite-Length Solutions for Rotordynamic Coefficients of Turbulent Annular Seals. J. Lubr. Technol., vol. 105, no. 3, 1983, pp. 437-445.

6. Allaire, P.E.; Lee, C.C.; and Gunter, E.J.: Dynamics of Short Eccentric Plain Seals with High Axial Reynolds Number. J. Spacecraft, vol. 15, no. 6, 1978, pp. 341-347.

7. Yang, B.S.; Iwatsubo, T.; and Kawai, R.: A Study on the Dynamic Characteristics of Pump Seal (1st Report, In Case of Annular Seal with Eccentricity). Bull. JSME, vol. 27, 1984, pp. 1047-1053.

8. Fleming, D.F.: Damping in Seals for Compressible Fluids. Rotordynamic Instability Problems in High-Performance Turbomachinery. NASA CP-2133, 1980.

9. Childs, D.W.; Dressman, J.B.: Convergent-Tapered Annular Seals: Analysis and Testing for Rotordynamic Coefficients. ASME Winter Annular Meeting, 1981, pp. 35-41.

10. Bolleter, U.; and Florjancic, D.: Predicting and Improving the Dynamic Behavior of Multistage High Performance Pumps. 1st Int. Pump Symposium, 1984, pp. 1-8.

11. Burton, R.A.: Approximation in Turbulent Film Analysis. J. Lubr. Technol., vol. 96, no. 1, 1974, pp. 168-173.

12. Komotori, K.; and Mori, H.: Leakage Characteristics of Labyrinth Seals. 5th Int. Conf. on Fluid Sealing, Paper E4, 1971.

13. Black, H.F.: On Journal Bearing with High Axial Flows in the Turbulent Regime. J. Mech. Eng. Sci., vol. 12, no. 4, 1970, pp. 301-303.

14. Hauck, L.: Exciting Forces due to Swirl-Type Flow in Labyrinth Seals. IFToMM Paper, 1982, pp. 361-368.

15. Black, H.F., et al.: Inlet Flow Swirl in Short Turbulent Annular Seal Dynamics. 9th Int. Conf. on Fluid Sealing, BHRA Fluid Enrg., 1981.

TABLE I. - NUMERICAL CALCULATION MODEL

Working fluid	Water
Fluid temperature, K	293.15
Density, ρ, kg/m^3	9.982×10^2
Viscosity, μ, mPa s	1.009
Kinematic viscosity, ν, m^2/s	1.006×10^{-6}
Journal radius, R, mm	100.0
Seal radial clearance, C_o, mm	0.4
Seal length, L, mm	55 to 205
Groove depth, T, mm	3.0
Divergent flow angle, θ, deg	4.0
Journal rotating frequency, N, rpm	2000 to 8000
Pressure difference, ΔP, MPa	0.49 to 4.9

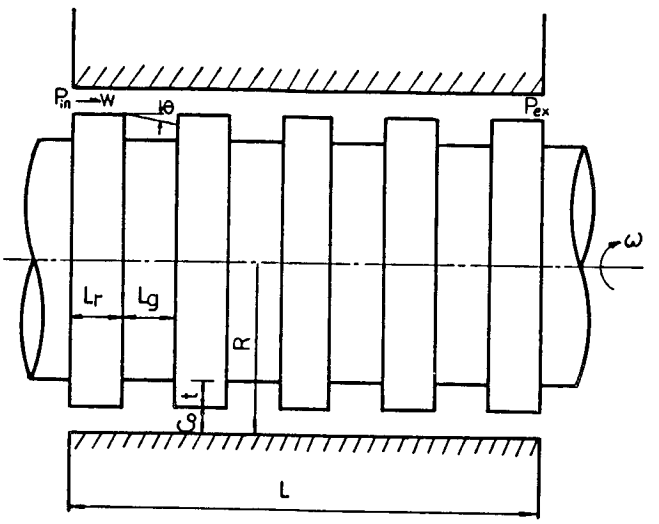

Figure 1. - Geometry of parallel-grooved seal.

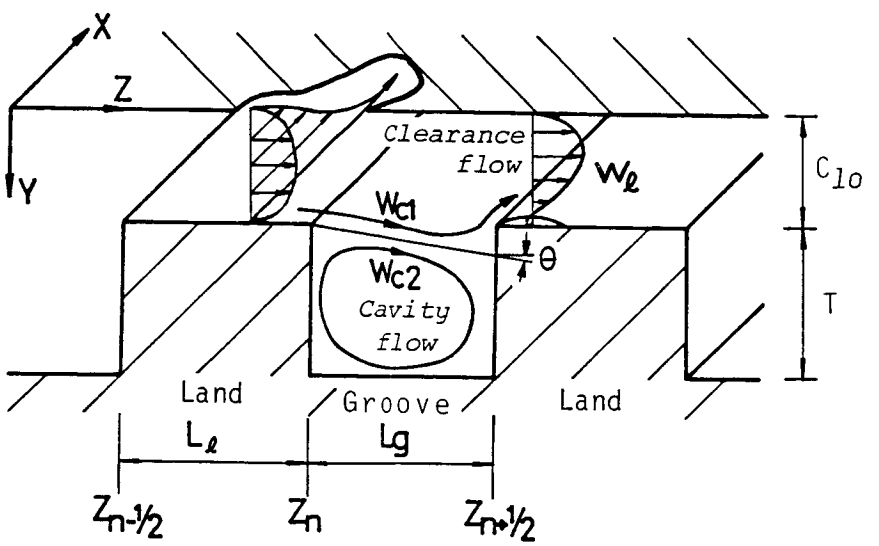

Figure 2. - Streamlines and coordinate system for seal analysis.

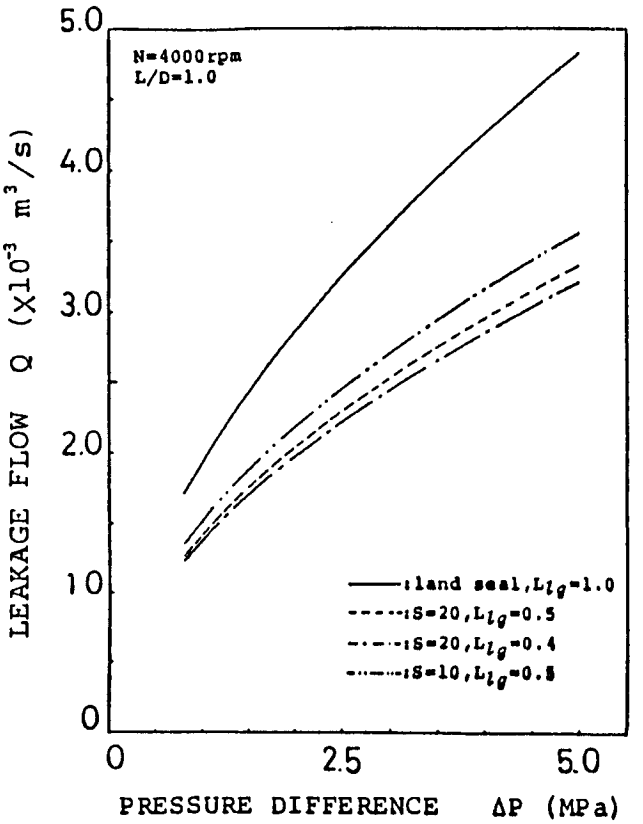

Figure 3. - Leakage flow rate.

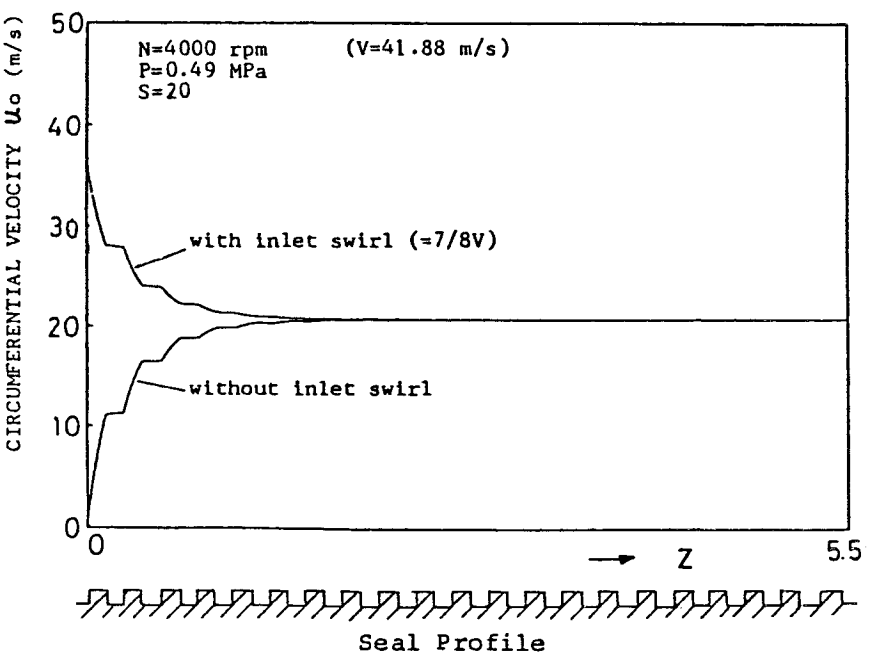

Figure 4. - Axial distribution of circumferential fluid velocity.

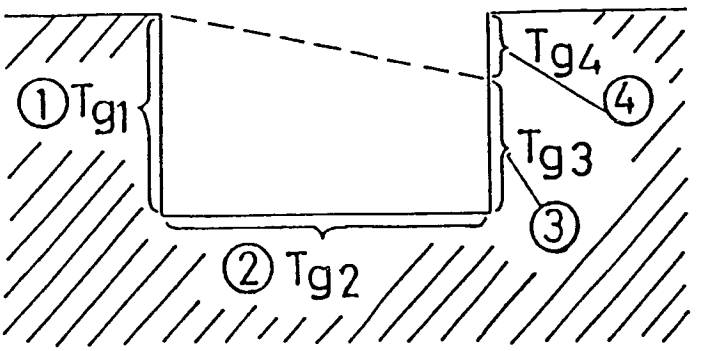

Figure 5. - Torque loss of groove.

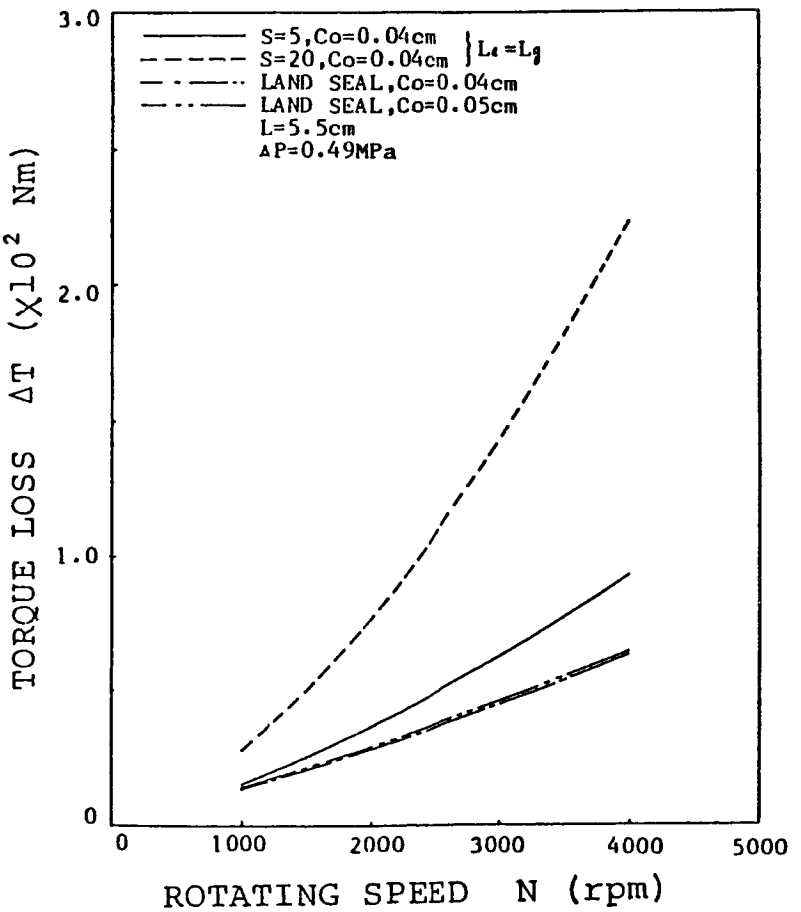

Figure 6. - Torque loss.

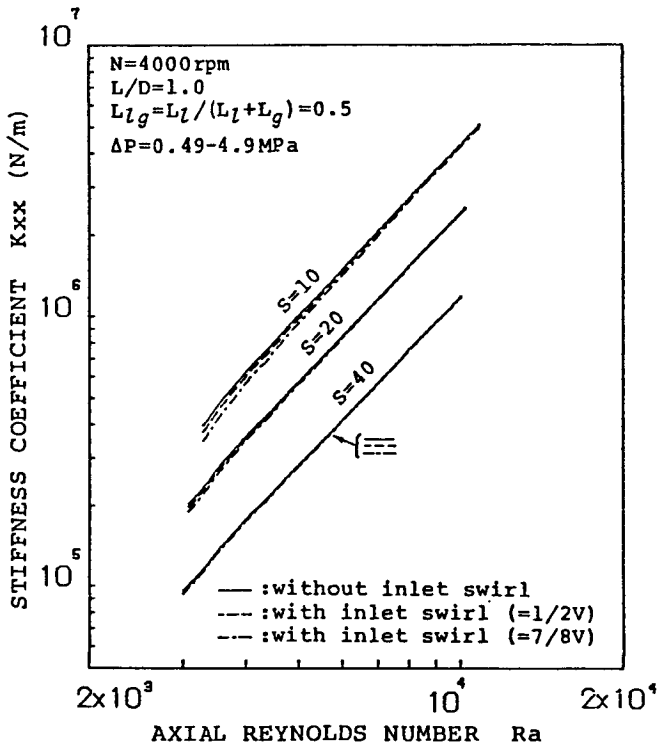

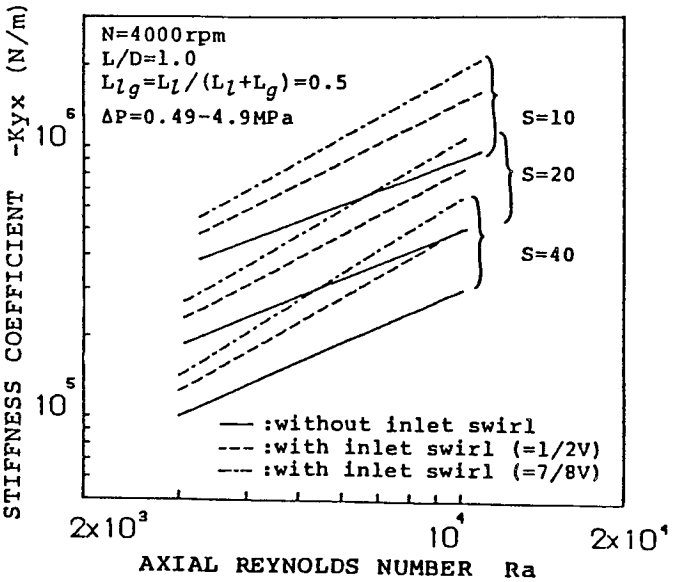

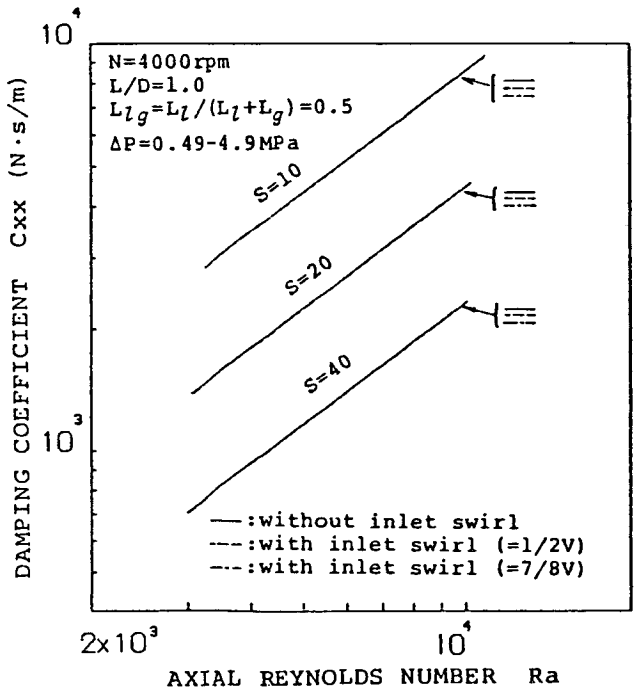

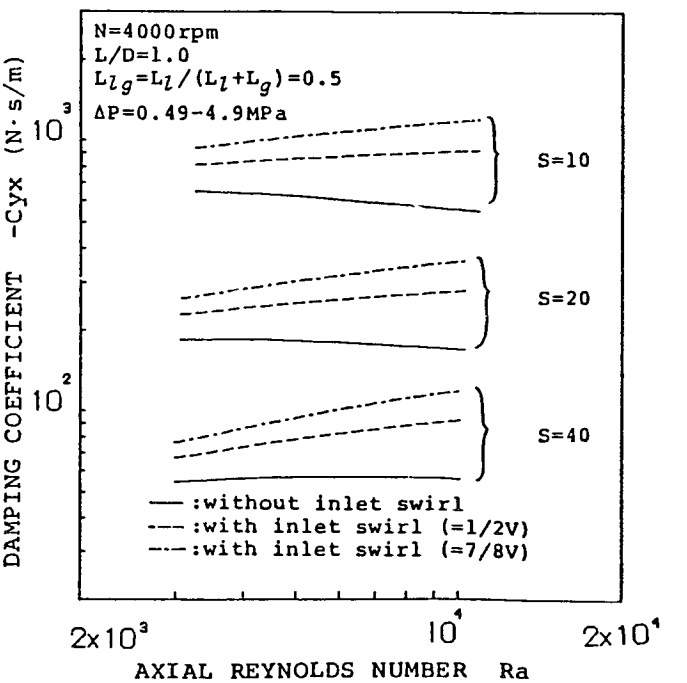

Figure 7. - Influence of number of stages.

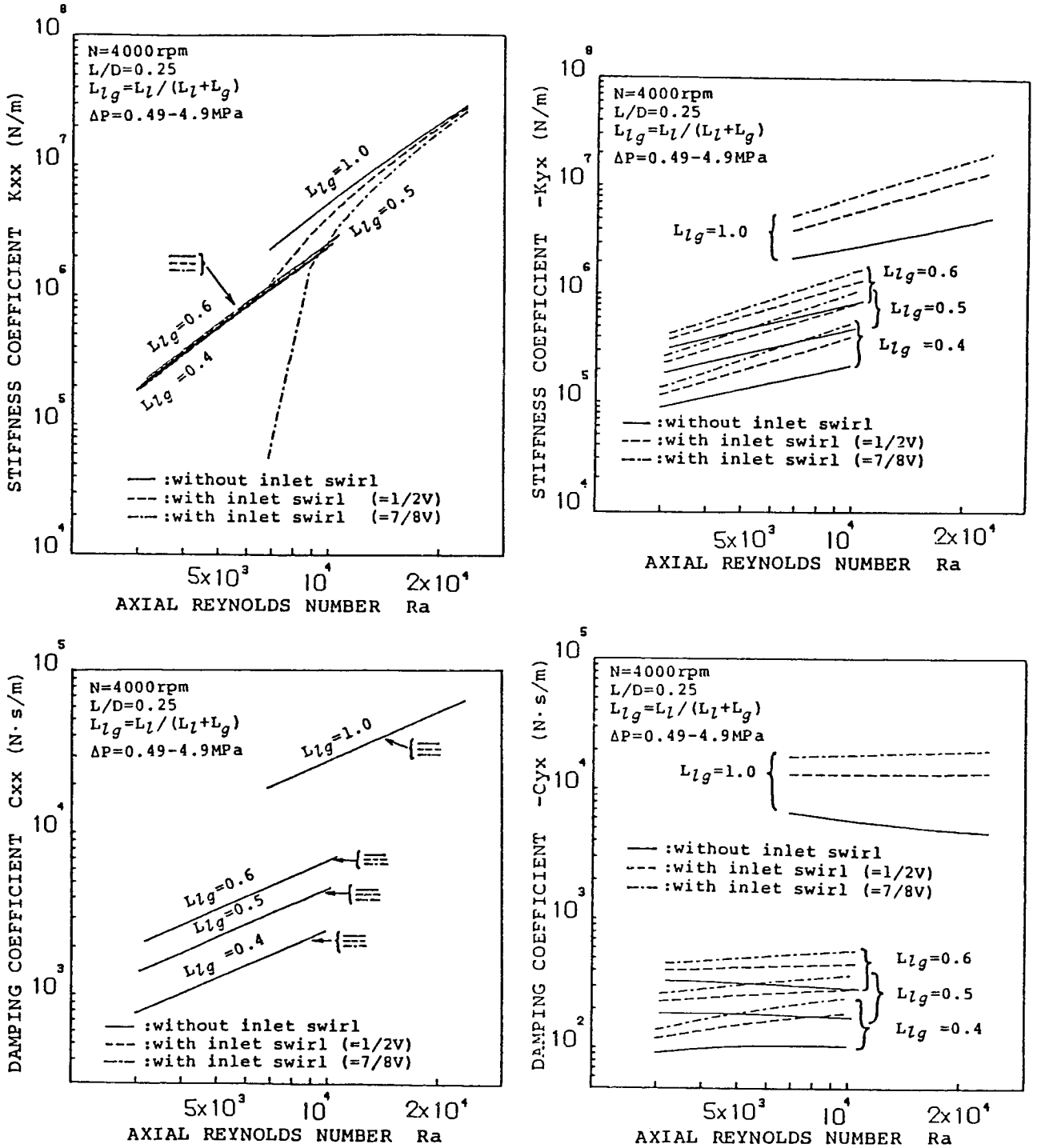

Figure 8. - Influence of ratio of land width to groove width plus land width L_{lg}.